Characterization and genotoxic effects of green synthesis zinc oxide nanoparticles mediated by Punica granatum peel extract and its antimicrobial activity

Abdelghany S. Shaban (abdelghanysobhy@azhar.edu.eg)
Al-Azher University
M. E. Owda
Al-Azher University
Mostafa M. Basuoni
Al-Azher University
M. A. Mousa
Al-Azher University
Ahmed A. Radwan
Al-Azher University
Ahmed K. Saleh
National Research Centre

Research Article

Keywords: Green synthesis, ZnO -NPS, Hordeum vulgare L, cytotoxicity, genotoxicity, and antimicrobial activity.

Posted Date: April 18th, 2022

DOI: https://doi.org/10.21203/rs.3.rs-1538694/v1

Abstract

Green synthesis of zinc oxide nanoparticles (ZnO-NPs) mediated fruit peel extract is gaining importance due to its cost-effectiveness and ecofriendly. Herein, ZnO-NPs were synthesized by pomegranate peel extract as a reducing and stabilizing agent. The synthesized ZnO-NPs were characterized using SEM, TEM-SAID, FT-IR, XRD and particle size analysis. The results revealed that the ZnO-NPs was agglomerated spherical and hexagonal shapes with an average diameter of 20 to 40 nm and crystallinity formed. For multiple applications of ZnO-NPs, the antimicrobial activity showed significant inhibition against the pathogenic microbes used with 62.5 and 31.25 µg/ml of MIC for both Gram-positive and Gram-negative bacteria respectively, 125 and 250 µg/ml of MIC for *Aspergillus niger* and *Aspergillus flavus*, respectively. Also ZnO-NPs showed antioxidant activity with IC_{50} = 240 and 250 µg/ml by DPPH and ABTS respectively. All concentrations of ZnO-NPs showed greatly significance for improved germination of barley seed and shoot height with the optimum concentration reach to 2 and 12 ppm of ZnO-NPs for both seed germination (90%) and shoot height (6.5) respectively, while the greatest root extension (6 cm) was observed at 2 ppm of ZnO-NPs.

The mitotic index increased at lower nanoparticle concentrations and exposure times but declined considerably as the nanoparticle dose and exposure duration increased, until most concentrations reached 100% suppression after 12 hours with a variety of chromosomal abnormalities. Using a green synthetic strategy, the researchers were able to create efficient, eco-friendly, and simple multifunctional ZnO NPs, and in the process, they gained a deeper understanding of the cytotoxicity and genotoxicity of ZnO-NPs in plant cells.

1 Introduction

Nanotechnology enables the development of unique nanostructures, the study of their novel features, and the application of these structures in a variety of domains of application [1]. Nanomaterials have made significant contributions to basic and applied sciences. Several approach can be used to synthesis nanoparticles like chemical, physical and green approach; however, green synthesis has gained popularity in recent years [2]. Green synthesis has a variety of advantages over standard chemical or physical techniques, including the requirement for mild reaction conditions, the use of less harmful ingredients, low cost, and ecofriendly [3]. Biological agents such as plant extracts, fruit extracts, and microorganisms are all employed in green synthesis [4].

Plant extracts enable the biological production of many metallic nanoparticles, which is more environmentally friendly and enables the regulated synthesis of nanoparticles with well-defined size and form [5–7]. "Power fruit" is a term coined to describe the pomegranate (*Punica granatum)*, a fruit that has been hailed for its remarkable medicinal capabilities and consumer health benefits [8]. After harvest, the peel of *P. granatum*. accounts for around one-third of the fruit's weight and is scraped off the fruit. Agro-waste from fruits has gained a lot of attention in recent years because of its abundant availability and inexpensive cost [9]. The high concentration of phenolic compounds in the peel of *P. granatum* has long

been recognised as a natural source of antioxidants [10]. In addition to punicalagin and the gallic and ellagic acids present in pomegranate peels, there are also chlorogenic acids, caffeic acids, punicalins and other phenolic compounds such as apigenin, quercetin, pelargonidin, granatin A and B [10]. The critical nature of using natural, renewable, and low-cost materials for avoiding the presence of toxic compounds and solvents, *P. granatum* used as green synthesis of metal oxide nanoparticles in an aqueous media [11–13].

On a global basis, zinc oxide nanoparticles (ZnO-NPs) are one of the most widely produced nanomaterials. Numerous industrial products, including sunscreens, cosmetics, and paints, contain these NPs [14, 15]. In a variety of plant species (including crops), ZnO-NPs at optimal concentrations used for improving seed germination and seedling growth [16, 17]. Additionally, ZnO-NPs have been proposed as a source of zinc (Zn) for plants [18]. Because metallic Zn is involved in a range of enzymatic and physiological activities, it is essential for plant growth and development [19]. Zn is required for protein, carbohydrate, and nucleic acid synthesis, as well as chlorophyll biosynthesis, energy production, and macromolecule metabolism, where it acts as an enzyme component, a catalyst, or a structural cofactor [20]. Zn increases seed germination, stimulates radical growth, regulates water absorption and transport capacity, and protects plants from the damaging effects of heat, drought, and salt stress. Additionally, Zn is necessary for the synthesis of plant hormones such as auxins and gibberellins [21–23].

Due to their propensity to absorb and gather nanoparticles from the soil, water, and air, plants are especially vulnerable to nanotoxicity. As a result, plants are frequently used as a model organism for assessing the potential toxicity of various nanomaterials [24, 25]. Barley (*Hordeum vulgare* L.) is the fourth largest cereal crop in the world and one of the most widely cultivated cereals for human and animal consumption [26, 27]. Barley has been effectively employed as a model organism for genetic studies due to its diploid nature and high genetic diversity [28, 29].

It has become a global concern that antimicrobial resistance (AMR) is on the rise. Apoptosis, a cell death caused by the oxidative stress caused by ZnO-NPs, is an effective way to stop bacterial growth and biofilm formation [30]. ZnO-NPs and conventional antibiotics can work synergistically against Acinetobacter baumannii resistance, according to a 2016 study by Ghasemi and Jalal [31]. ZnO-NPs were found to enhance the absorption of antibiotics by enhancing bacteria's ability to metabolise them [30].

The aim of this study was conducted for green synthesis of ZnO-NPs using pomegranate peels extract and their physicochemical characterizations. This nanoparticle was evaluated for their antimicrobial and antioxidant activates, as well as, seed germination, root, shoot length and cytogenetics effects of ZnO-NPs were investigated in vitro.

2 Material And Methods:

2.1. **Materials**

Zinc nitrate [$Zn(NO_3)_2 \cdot 6H_2O$] as the source of Zn^{2+},sodium hydroxide and ethanol was purchased from sigma, Seeds of barley were obtained from Egypt's Ministry of Agriculture.

2.2. Methods

2.2.1 Pomegranate peels (POP) extraction

Pomegranate (*Punica granatum*) fruit was provided from the local market in Egypt, this fruit was washed well by clean tap water to remove extraneous materials and the peels and seeds were separated manually. The POP extract was prepared by the method described by [32] with little modifications. The fresh POP (100 gm) were cut into small pieces and ground in 500 ml distilled water by high-speed blender (800ES blender, 230 volt, 50 HZ, 330 Wt, model BB90E, USA) for 10 min at room temperature. The dispersed POP mixture was boiled for 45 min under steered conditions. Then, the mixture was centrifuged at 15000 rpm for 15 min at 4°C and the supernatant of POP extracts filtered, collected, and kept at 4°C for further used [32].

2.2.2 Green synthesis of ZnO-NPs

Zinc nitrate hexahydrate [$Zn(NO_3)_2 \cdot 6H_2O$] and aqueous extract of POP were used in a 1:20 ratio for the green route production of ZnO-NPs. 1M NaOH was added drop by drop to adjust pH from (8–12) and stirred for 2 hours at 100°C, yielding a yellowish precipitate. To separate this precipitate, the solution was cooled and centrifuged at 10,000 rpm, then washed several times with distilled water and ethanol to remove dust particles. After that, a solid powder was obtained and dried in a 60°C oven. The product was calcined for 4 hours at 450°C in a muffle furnace (Fig. 1).

2.2.3 Characterization of ZnO-NPs

The Fourier Transform Infrared Spectroscopy (FT-IR) were measured using a Spectrum 100 spectrophotometer (Perkin Elmer Inc., USA) in a total-reflection mode. The measurements were performed from 4000 to 250 cm^{-1} at a resolution of 4 cm^{-1}. Scanning Electron Microscope (SEM) (Philips, model Quanta Feg 250) was used to monitor the fracture surface of the films. The samples for SEM analysis were coated with a layer of gold and were imaged at an operating voltage of 20 kV under vacuum. Samples were observed under transmission electron microscopy (TEM) on JEOL (GEM-1010) at an operating voltage of 76 kV. X-ray diffractometer (XRD) was measured by (PANa-lytical, Netherlands) at 25°C with Cu Kα a monochromatic radiation source (λ = 0.154 nm, 2θ = 5°: 80°, and scanning time 5 min).

2.2.4 Antimicrobial Activity

The antimicrobial activities of biosynthesized ZnO-NPs against pathogenic microbial strains, Gram positive bacteria *Bacillus cereus* ATCC 10,987 (*B. cereus*) and *Staphylococcus aureus* ATCC 6538 (*S. aureus*), Gram negative bacteria *Escherichia coli* ATCC 8739 (*E. coli*) and *Klebsiella pneumonia* ATCC 13,883 (*K. pneumonia*), and multicellular fungi *Aspergillus niger* (*A. niger*) and *Aspergillus flavus*(*A. flavus*) was evaluated under aseptic conditions, using Muller Hinton agar for bacteria and Potato

dextrose agar for fungi by agar well-diffusion technique. All bacterial used were obtained from American Type Culture Collection (ATCC).At concentration 1000 μg/ml, about 100 μl of biosynthesized ZnO-NPs nanofluid was used and 100 μl of base fluid was also used as negative control. In addition, Azithromycin (15 ug/ml) was used as antibiotic control for the bacteria and fluconazole powder (25 ug/ml) used as antifungal control. All plates were placed in refrigerator for 2 h to inhibit the microbial used and allow the tested compounds to diffuse. Then bacteria were incubated at 37°C for 24 h. and fungi at 28°C for 72–96 h. At the end of the incubation, the zone of the inhibition by mm was measured [33].

The MIC (minimum inhibitory concentration) of the biosynthesized ZnO-NPs nanofluid was estimated, using concentrations starting from 500 ug/ml and diluted double-fold to 7.8 ug/m [34]. Each trail was repeated in triplicate.

2.2.5 Antioxidant activity

2.2.5.1 DPPH assay

Antioxidant activity of ZnO-NPs was carried out using DPPH (2,2-diphenyl-1-picrylhydrazyl) method according to Sharaf *et al* [35]. The DPPH method was modified to evaluate the scavenging activity of ZnO-NPs on free radicals. DPPH reagent was prepared by dissolved 8 mg of DPPH in 100 ml of MeOH. The scavenging activity of ZnO-NPs was done by mixed 100 μL DPPH reagent with 100 μL of ZnO-NPs in a well of micro plate then incubated for 30 min at room temperature. After that, the plate was measured at 490 nm using an ELISA plate reader (TECAN, Austria), The scavenging activity for free radicals by ZnO-NPs was calculated as following:

$$\mathrm{DPPHscavengingactivity} = \frac{\mathrm{controlabsorbance} - \mathrm{ZnNPsabsorbance}}{\mathrm{controlabsorbance}} \mathrm{X100}$$

Different concentrations of ZnO-NPs (1000, 500, 250, 125, 62.5, 31.25, 15.6 and 7.8 µg/ml) were used to determine their DPPH scavenging activity. Antioxidant activity of ascorbic acid as standard and ZnO-NPs was estimated. The IC_{50} values (the concentration of tested material required for inhibit 50% of DPPH radicals)

2.2.5.2 ABTS Assay

Another assay used to evaluate the antioxidant activity was ABTS (2,2'-azino-bis(3-ethylbenzothiazoline-6- sulfonic acid) according to the modified method used by Lee [36].

$$\mathrm{APTSscavengingactivity} = \frac{\mathrm{controlabsorbance} - \mathrm{ZnO-NPsabsorbance}}{\mathrm{controlabsorbance}} \mathrm{X100}$$

2.2.6 Evaluation of ZnO-NPs for seed germination and length of root and shoot

Seeds of barley (Hordeum vulgare) were obtained from Egypt's Ministry of Agriculture. To assure the sterility of the surface, healthy and uniform barley seeds were immersed in a 1% sodium hypochlorite solution for 5 min and then rinsed three times with distilled water. At 25°C, seeds germinated on filter sheets soaked with ZnO-NPs (1, 2, 4, 8, and 12 mg/L) and distilled water as a negative control. Each treatment consisted of five duplicates of ten seeds. The number of seedlings was counted after four days of treatment to determine the germination percentage, once seeds germinate, a 2-mm radicle grows from them. Percentage of germinated seeds equals the number of germinated seeds divided by the total number of seeds. Regular measurements of shoot height and root length were taken until the tenth day.

2.2.7 Evaluation of ZnO-NPs for cytotoxicity and genotoxicity

Seeds of barley were germinated on moistened filter sheets with distilled water until the roots attained a length of approximately 1 cm. Roots were subjected to previously determined concentrations for 3, 6, 9, and 12 h, with three duplicates for each treatment. After 24 h of fixation in ethanol: acetic acid (3:1), the roots were hydrolyzed for 10 min in a water bath at 60°C with 1 N HCl. The root tips were then dyed using the Feulgen squash process [37]. To determine the mitotic index (MI) and chromosomal aberrations, a minimum of 2000 cells from the control and all treated groups were scored using an optical microscope at a magnification of 40. The MI % is computed by dividing the total number of dividing cells by the total number of cells counted. The percentage of phase index is computed by dividing the total number of dividing cells seen by the number of cells in each phase. By counting cells at various stages of mitosis, the overall chromosomal abnormality percentage (CA, number of cells with chromosomal abnormalities/number of cells in division 100) was determined. The researchers counted micronuclei (MN) that were smaller than a third the diameter of the major nucleus. The frequency of MN was calculated using the number of cells with micronuclei per 1000 scored interphase cells [38].

3 Results And Discussion

3.1 Characterization of green synthesized ZnO-Nps

3.1.1 SEM and TEM analysis

SEM measurement was carried out to analyze the morphology of ZnO-NPs. The SEM images (Fig. 2a) show that, the produced ZnO-NPs are nearly spherical in shape with agglomeration due to their water interaction and the intramolecular Van der Waals, magnetic and electrostatic interactions. The nanoscale and uniformity of ZnO-NPs are revealed by TEM images. The shape of the nanoparticles produced is of a spherical nature with an average size found to be 20 to 40 nm as shown in the (Fig. 2b). The SAED pattern in Fig. 2c indicates that the biosynthesized ZnO-NPs were polycrystalline in nature. The particle size distributions for the sample are shown in the (Fig. 2d). Low polydispersity index values indicate that the particles are homogeneous and have direct spherical forms (confirmed in the SEM analysis). Particle

size distributions cover a small range of particle diameters and the smallest particles in the sample had diameters ranging from 1 to 550 nm, with an average size diameter of 122.6 nm [39].

3.1.2 FT-IR and XRD analysis

Figure 3a shows the FT-IR spectrum of ZnO-NPs. The presence of organic compounds in the sample is associated to absorption peaks in the region of 800–1600 cm^{-1}. The stretching vibration band of C = O of the amide group and the presence of carboxyl (COOH) and hydroxyl (OH) groups are shown by the absorption peaks at 1630.12 cm^{-1} and 3437.05 cm^{-1}, respectively [40], while the -CH_2- and C-C in the aromatic ring are responsible for the peaks at 2920.46 cm^{-1} and 1411 cm^{-1}, respectively. Stretching vibrations of C = O can also be attributed to the absorption peaks at 1630 cm^{-1}. The presence of phenolic groups, alcohols, and aliphatic amines is also indicated by a peak at 1039.81cm^{-1}. The phenols in the capping agent bond to the surface of ZnO and cause ZnO NPs to form, while the C = O, C = O–C and C = C groups of heterocyclic compounds may act as a stabilizer [41, 42]. Then FT-IR spectrum absorbs the peak at 875.38 cm^{-1} indicate the stretching vibrations of ZnO because the peaks in the range from 500–900 cm^{-1} are attributed to metal Oxide bonds [43]. Using XRD analysis is useful tool to determine the phase and crystalline nature of ZnO nanoparticles. In the current study, XRD pattern of ZnO-NPs (Fig. 3b) showed different peaks at (2Θ) = 31.75 (1 0 0), 34.46 (0 0 2), 36.32 (1 0 1), 47.46 (1 0 2), 56.63 (1 1 0), 62.75 (1 0 3), 66.36 (2 0 0), 68.13 (1 1 2) and 69.10 (2 0 1) which agree with the JCPDS card (NO 36–1451) for a typical hexagonal phase of wurtzite form crystalline material [44, 45]. The presence of (1 0 0), (0 0 2), (1 0 1) planes in XRD designates the formation of hexagonal phase of wurtzite structure of ZnO-NPs. No impurity peaks were noted indicated the formation of pure ZnO-NPs. The prominent sharp peak at (101) represents the polycrystalline structure of ZnO-NPs. The average crystalline size was found to be 22 nm which was further confirmed by TEM analysis and SAED. These results are in accordance with previous studies on ZnO-NPs synthesized using leaf extract of *Tecoma castanifolia* [43] and *Conyza canadensis* [46].

3.2 Antimicrobial activity of ZnO-NPs

The antimicrobial effect of biosynthesized ZnO-NPs can be interpreted to different actions such as (1) generating reactive oxygen species (ROS), (2) ZnO-NPs and cell walls of microbes interaction that finally causes oxidative stress and death of cells, (3) electrostatic attraction the microbial cell and (4) entry of Zn^{2+} ions into the cell, [47, 48].

The ZnO-NPs nanofluid inhibit the growth of all tested pathogenic microorganisms, with antimicrobial activities by diameters ranged from 19.7 ± 0.29 to 24.6 ± 0.32 mm at concentration 1000 ug/mL as showed in Table 1 and Fig. 4, ZnO-NPs exhibit inhibition effect against Gram-negative bacteria more than Gram-positive bacteria and fungi, there is no effect for base fluid against any of the tested microorganisms, which proved that the antimicrobial activity of ZnO-NPs, different inhibition zone results for antibiotic controls were recorded which less than that obtained fromZnO-NPs.

The detect of MIC values of biomolecules against pathogenic microorganisms especially if these biomolecules are integrated into medical applications had a significant value. Effect of different concentration of ZnO-NPs (500, 250, 125, 62.5, 31.25, 15.6 and 7.8 µg/ml) against tested microbes showed that, the MIC value for Gram-positive bacteria (*B. cereus* and *S. aureus)* were 62.5 µg/ml; Gram-negative bacteria *(E. coli* and *K. pneumonia)* were 31.25 µg/ml, while MIC value for *A. niger* and *A. flavus* were 125 and 250 µg/ml respectively.

In the current study, Gram negative bacteria (*E. coli*) was the most sensitive microbes toward biosynthesized ZnO-NPs, and this action can be due to differences in cell wall structures between Gram negative and Gram-positive bacteria. The Gram-negative bacterial cell wall was distinguished by a thin layer of peptidoglycan and lipopolysaccharides (LPS). The positive charge of ZnO-NPs is hardly adhesive to the negative charge of LPS, and hence it is the adsorbed on the Gram-negative bacterial cell membrane that ultimately disrupts selective permeability [49]. Moreover, the inhibition effect of ZnO-NPs on fungi significantly deform conidial formation and conidiophores of *Penicillium expansum* and *Botrytis cinerea*, displaying antifungal properties [48, 50].

Table 1
Antimicrobial activity and MIC values of biosynthesized ZnO-NPs.

No.		**Mean Diameter of Inhibition Zone (mm) _ Std. Error**			
	Microorganisms	ZnO-NPs	Base fluid	Antibiotic control	MIC (ug/mL)
1	*B. cereus*	19.7 ± 0.29	0.0	22.3 ± 0.34	62.5
2	*S. aureus*	17.9 ± 0.51	0.0	22.1 ± 0.45	62.5
3	*E. coli*	24.6 ± 0.32	0.0	17.2 ± 0.61	31.25
4	*K. pneumonia*	22.3 ± 0.25	0.0	18.7 ± 0.42	31.25
5	*A. niger*	23.3 ± 0.49	0.0	19.6 ± 0.35	125
6	*A. flavus*	21.7 ± 0.22	0.0	18.6 ± 0.57	250

3.3 Antioxidant activity of ZnO-NPs

Antioxidant activity has been found in a wide range of natural and artificial substances [51]. Antioxidant activity was assessed using DPPH radical-scavenging activity and ABTS radical-scavenging activity tests in the current study. Antioxidants are chemicals that neutralise ROS which are formed as a byproduct of biological events [52]. Several antioxidant qualities, including anti-atherosclerosis, anti-inflammatory, anti-tumor, anticancer, anti-mutagenesis, anti-carcinogenesis and anti-microbiosis, have led to their use as therapeutic agents (Fig. 5). In recent study, the antioxidant activity of ZnO-NPs was evaluated using DPPH and ABTS assays, as shown in Fig. 1. Results proved that the antioxidant activity of ZnO-NPs with IC_{50} = 240 µg/ml compared to 16.2 µg/ml for ascorbic acid in the case of DPPH, while IC_{50} of ZnO-NPs and ascorbic acid using ABTs assay were 250 and 1.6 µg/ml, respectively.

3.4 Evaluation of ZnO-NPs for seed germination

Short-term phytotoxicity of emerging contaminants, such as designed NPs, can be estimated using seed germination and root/shoot elongation experiments [53]. In this study, germination was defined as the radicle or plumule emerging from the seed coat. The germination of barley seeds exposed to ZnO-NPs was assessed after 4 days of treatment. ZnO-NPs treatment demonstrated a positive effect on barley seeds when compared to the control. The seed germination of barley was significantly increased at all ZnO-NPs doses examined. The seedlings germinated with the addition of ZnO-NPs at 2 mg/l had the highest germination rate (90%), while the control seeds had a considerably lower germination rate (63%). At 1, 4, 8, and 12 PPM of ZnO-NPs, the seed germination rate was record 83, 67, 77, and 83%, respectively (Fig. 6a). Germination of the seeds began after one day, with a proportion ranging from 60% under 1 and 2 PPM ZnO-NPs conditions to 50% under control. Zn is an important plant micronutrient that is frequently supplemented with zinc sulphate in agricultural practices to prevent Zn deficiency. Our findings resembled those of Plaksenkova et al. [54], who reported that low ZnO-NPs concentrations of 1,2, and 4 PPM significantly increased barley seed germination. In addition Upadhyaya, [55] recorded an increase in the germination of rice seeds treated with Zn NPs, which is consistent with our findings. In contrast to Xiang et al. [53], ZnO-NPs at concentrations of 1–80 mg/l had no influence on Chinese cabbage seed germination when compared to the control. Raliya et al. [56] also reported that ZnO-NPs had no influence on tomato seed germination at concentrations up to 750 mg/kg. According to Zhang et al [57], ZnO-NPs at concentrations of 10, 100, and 1,000 mg/l had no statistically significant effect on maize or cucumber germination, suggesting that germination rate is species- and concentration-dependent.

3.4 Assessment of ZnO-NPs for root and shoot length

In plants, Zn acts as a cofactor for RNA polymerases and other plant enzymes, influencing their activity. Phosphorus mobilisation enzymes such as phosphatase and phytases are stimulated by ZnO-NPs in the rhizosphere, increasing the amount of phosphorus available to plants [58, 59]. ZnO-NPs has a dual role as essential nutrients and native phosphorous mobilizers is supported by the improved physiological and biochemical responses. [60].

Both root and shoot length were influenced by ZnO-NPs as showed in (Fig. 6b). The difference in root elongation between control and all ZnO-NPs concentrations was substantial (Fig. 6b). At 2 PPM ZnO-NPs concentration, the maximum root elongation was 6 ± 1.2 cm, while the control plants' root length was 3.6 ± 1.2 cm. At a concentration of 12 PPM ZnO-NPs, the minimum root length was found to be 3.1 ± 1.3 cm. According to previous controlled studies, the toxicity of NPs during the early stages of plant growth is most likely due to the following factors: I chemical and physical properties that affect the release of ions or the aggregation of particles into more stable forms; and (ii) particle size and shape, which determine the specific surface area of NPs [61, 62]. A quick and commonly used acute phytotoxicity test method, seed germination and root elongation, has various advantages, including sensitivity, simplicity, cheap cost, and applicability for unstable substances or samples [63, 64].

The effects of suspended ZnO-NPs on young shoots are seen in (Fig. 6b). There was a positive reaction in shoots, with ZnO-NPs at all concentrations promoting significant increases in shoot length, which increased progressively as concentrations increased. At 12 PPM of ZnO-NPs concentration, the highest shoot elongation was 6.5 ± 1.2 cm, compared to 3.2 ± 0.8 cm for the control shoot. Most concentrations of ZnO-NPs (1,2,4 and 8 mg/l) in our investigation encouraged root and shoot growth in contrast to control, with the exception of 12 PPM, where root growth was similar to control. ZnO-NPs at a concentration of 10 mg/l greatly increased the root length of germinated maize, according to [58]. Our results were similar to those of Plaksenkova et al. [54], who found that low ZnO-NPs concentrations of 1, 2, and 4 PPM improved barley root and shoot lengths considerably.

Root and shoot length in tomato (*Lycopersicon esculentum* L.) plants treated with ZnO-NPs at doses of 2, 4, 8, or 16 mg/l were longer than in control plants, [61]. Furthermore, lower ZnO-NPs concentrations (10 and 20 mg/l) resulted in a significant increase in onion seedling shoot and root lengths, but higher concentrations (30 and 40 mg/l) resulted in a significant decrease in onion seedling shoot and root lengths [62]. In contrast to Munzuroglu and Geckil. [63], a wide range of ZnO-NPs concentrations, from low (50 mg/l) to very high (3200 mg/l), had no effect on the length of three-week-old onion plantlets grown in vitro.

On the other hand, Wang et al. [64] reported that, the ZnO-NPs suppressed garlic root growth as concentration increased. At a concentration of 50 mg/l, ZnO-NPs completely stopped root development. Low ZnO-NPs concentrations cause an increase in root and shoot length, which could be a nutritional benefit of nano zinc oxide. Zn content in seeds plays an important physiological role during seed germination and early seedling growth [65]. Zn also aids elongation and cell division by stabilising indole-3-acetic acid, the most common auxin in plants when collected in significant concentrations, however, it is hazardous due to its episodic binding to proteins and subsequent displacement of other metal ions, notably Fe [66, 67].

Finally, Variations in plant responsiveness to ZnO-NPs application may be attributed to genotype, plant part/organ (treatment of seeds, roots or leaves), experiment environment (in vitro or in vivo), NP features (size, shape and concentration), and/or exposure time [68].

3.5 Effect of ZnO-NPs on MI

In genotoxicity studies, cytogenetic analysis of root meristems with an optical microscope is a quick and effective way to determine the MI, chromosome breakages and anomalies, micronuclei [69], spindle failure, and polyploidy and aneuploidy occurrence [70, 71].The cytotoxicity and genotoxicity capacity of ZnO-NPs on barley seedlings was estimated using cytological indicators such as the MI, the number and percentage of chromosomal abnormalities. Tables 1 and 2 illustrate the cytological and chromosomal abnormalities seen in the root tip cells of barley treated with various doses of ZnO-NPs.

The control sample had a MI of 5.67 ± 0.04 and normal divisional phases, with the exception of a minor number of aberrant cells at prophase (3.53 ± 0.01). The percentage of dividing cells increased

significantly until 8 mg/l ZnO-NPs was added, after which the value dropped significantly. The value of the MI (1.25 ± 0.07%) was lowered by nearly 4% at a dose concentration of 12 PPM compared to the control. This higher rise in MI at lower concentrations (1 and 2 PPM) was limited by short time exposure (3 and 6 h), but subsequent increases in nanoparticle dosage and time resulted in a significant decrease in MI until total suppression was achieved at 12 h with 4, 8, and 12 PPM concentrations. MI levels at all concentrations decreased with time as a result of long-term exposure as presented in Table 2 and Fig. 7. These results were constant with results reported by the Plaksenkova et al. [54], where the cytotoxicity generated by ZnO-NPs depend on their concentration and timeexposure. Also, there was a concentration-dependent decrease of MI in *V. faba*, indicating that ZnO-NPs have cytotoxic potential, according to [72].

According to our findings, exposing barley roots to ZnO-NPs produces cytotoxicity and genotoxicity. Table 2 summaries the mitotic parameters recorded before and after nanoparticle treatment. ZnO-NPs caused significant alterations in MI and a rise in chromosomal aberrations (Fig. 7) as a clear dose response impact, even when plants were exposed at low concentrations of them over a short period of time, according to the tests. CAs revealed that mitotic inhibition was linked to the gradual production of several chromosomal abnormalities.

The maximum value of MI (8.93 ± 0.06) was observed that the 3h for treatment with 1 PPM of ZnO-NPs, while the lowest (1.23 ± 0.01) was found at the 9 h for treatment with 12 PPM of ZnO-NPs. For a 12 h treatment at two doses, the drop in MI was statistically extremely significant, with a minimum value of 1.73 ± 0.06 and 1.25 ± 0.07% for (1 and 2 PPM ZnO-NPs, respectively) and complete inhibition for the other dosages. We may deduce that, the increased exposure period, ZnO-NPs concentration, and lower mitotic activity are all linked. Prophase was the most significant mitotic stage for all of the exposure doses examined, except for when 2 PPM was applied for 9 h and metaphase was the most abundant 90 ± 0.07 (Table 2 and Fig. 7).

The obtained results are in agreement with Giorgetti et al. [72], who used different ZnO-NPs treatments induce distinct increases in MI values in the *V. faba* root cell, with the lowest dosage (10 mg/l) causing the greatest rise. Previous research (73–75], showed that the MI values in the root tips of *A. cepa* and *V. faba* dropped when the concentration of Zn or ZnO-NPs and exposure length rose.

These suppression of MI with concentration dependent, indicating that ZnO-NPs have cytotoxic potential in barley. Kumari et al. [76] and Youssef and Elamawi. [77], described similar effects on MI, where *A drop* in the MI was seen as the nanoparticle concentration increased. Since ZnO-NPs appear to have a mitodepressive effect, this suggests that they may interfere with mitosis' natural development, preventing some cells from entering prophase and stopping the mitotic cycle in the interphase, therefore limiting DNA/protein synthesis [78, 79].

Table 2
Exposure to ZnO-NPs at different concentrations and for different durations of time affected the MI and phase index.

Time (h)	Conc. (PPM)	MI ± S.E	Mitotic phases % (Phase index %)			
			Prophase	**Metaphase**	**Anaphase**	**Telophase**
	control	5.67 ± 0.04	39.28 ± 0.03	47.67 ± 0.06	9.33 ± 0.04	3.52 ± 0.05
3	1	8.93 ± 0.01**	44.58 ± 0.04	43.37 ± 0.02	9.63 ± 0.03	2.42 ± 0.01
	2	8.63 ± 0.05**	49.20 ± 0.08	44.45 ± 0.01	6.35 ± 0.02	0
	4	3.25 ± 0.02*	59.09 ± 0.03*	36.36 ± 0.01*	2.28 ± 0.04**	2.27 ± 0.01
	8	3.47 ± 0.03*	41.91 ± 0.02	47.06 ± 0.04	8.72 ± 0.01	2.30 ± 0.02
	12	2.79 ± 0.05**	56.60 ± 0.04*	35.85 ± 0.07*	7.55 ± 0.01	0
6	1	7.69 ± 0.02**	92.30 ± 0.08**	7.70 ± 0.01**	0	0
	2	8.55 ± 0.03**	55.00 ± 0.02*	45.00 ± 0.01	0	0
	4	3.87 ± 0.05*	58.33 ± 0.06*	30.00 ± 0.03*	8.33 ± 0.02	3.34 ± 0.01
	8	3.07 ± 0.04*	34.62 ± 0.05	50.00 ± 0.01	15.38 ± 0.03**	0
	12	2.60 ± 0.05**	50.00 ± 0.03*	38.09 ± 0.02*	11.90 ± 0.01	0
9	1	3.23 ± 0.03*	51.51 ± 0.01*	36.37 ± 0.05*	9.09 ± 0.01	3.03 ± 0.01
	2	2.50 ± 0.04**	5.00 ± 0.02**	90.00 ± 0.07**	5.00 ± 0.03*	0
	4	3.02 ± 0.05**	48.78 ± 0.03	31.70 ± 0.02*	17.08 ± 0.04*	2.44 ± 0.01
	8	1.87 ± 0.02**	56.67 ± 0.01*	33.33 ± 0.03*	10.00 ± 0.02	0
	12	1.23 ± 0.01**	52.18 ± 0.04*	38.28 ± 0.01*	4.77 ± 0.03*	4.77 ± 0.02*
12	1	1.73 ± 0.06**	52.70 ± 0.03*	44.60 ± 0.03	0	2.70 ± 0.05

[1] S. E., Standard Error * Significant at level P < 0.05 ** Significant at level P < 0.01

2	1.25 ± 0.07**	70.00 ± 0.01**	30.00 ± 0.01*	0	0
4	**No divided cells (Full inhibition)**				
8					
12					

[1] S. E., Standard Error * Significant at level P < 0.05 ** Significant at level P < 0.01

3.6 Effect of ZnO-NPs on Chromosomal Aberration

Changes in chromosome structure caused by a break or exchange of chromosomal material are known as chromosomal aberrations. With varied quantities of ZnO-NPs suspensions, Multiple chromosomal abnormalities were found to be caused at all phases of the cell cycle, as well as changes in mitotic stages and nuclear membrane damage, according to the findings.

As the exposure length or ZnO-NPs concentration rose, the rate of chromosomal abnormality increased. For all concentrations tested, the percentage chromosomal aberration values were stated to be higher. At higher nanoparticle dosages of 12 PPM with all-time exposure and at lesser nanoparticle dosages with extended time exposure of 12 h, aberrant chromosomes were observed with their maximum percentage abnormality of 100% (Table 3). Increases in the percentage of abnormalities in root meristems indicate that the test substances are genotoxic [80]. Increased chromosomal abnormalities can be caused by a variety of reasons. The most significant is due to chemical interference during DNA repair. The clastogenicity of chemicals/nanoparticles is represented by many forms of chromosomal abnormalities.

Bridges, lagging, fragmented, disordered, micronucleous, and sticky chromosomes were found in the root meristem of barley that had been minimally exposed to various concentrations of ZnO-NPs as the most common abnormal cells (Table 3 and Fig. 8). When the total number of CAs was considered, the most common anomaly was irregular prophase, which had a high incidence in cell division stages followed by Stickiness and C-mitosis as the most common anomaly. The higher percentage from these CAs was recorded at the 2 PPM concentration as (88.18 ± 0.03 and 88.99 ± 0.04, respectively) (Table 3 and Fig. 8).

Table 3
percentage of abnormalities in all mitotic phases in barley root tips after treatment by different concentrations from ZnO-NPs.

Time (h)	Conc. (PPM)	Total abnormal cells (X ± S.E)	Abnormal mitotic phases %			
			prophase	Metaphase	Anaphase	Telophase
	control	3.53 ± 0.01	3.53 ± 0.01	0	0	0
3	1	72.29 ± 0.05**	38.55 ± 0.07**	25.30 ± 0.06**	6.02 ± 0.02*	2.42 ± 0.04
	2	100.0 ± 0.00**	49.20 ± 0.08**	44.45 ± 0.01**	6.35 ± 0.02*	0
	4	81.82 ± 0.05**	43.18 ± 0.02**	36.36 ± 0.01**	2.28 ± 0.04	2.27 ± 0.01
	8	91.39 ± 0.04**	37.07 ± 0.03**	44.61 ± 0.05**	7.95 ± 0.03*	2.30 ± 0.02
	12	100.0 ± 0.00**	56.60 ± 0.04**	35.85 ± 0.07**	7.55 ± 0.01*	0
6	1	72.30 ± 0.04**	64.60 ± 0.02**	7.70 ± 0.01**	0	0
	2	100.00 ± 0.01**	55.00 ± 0.02**	45.00 ± 0.01**	0	0
	4	91.67 ± 0.03**	51.67 ± 0.05**	28.33 ± 0.02**	8.33 ± 0.02*	3.34 ± 0.01*
	8	100.0 ± 0.00**	34.62 ± 0.05**	50.00 ± 0.01**	15.38 ± 0.03**	0
	12	100.0 ± 0.00**	50.00 ± 0.03**	38.09 ± 0.02**	11.90 ± 0.01*	0
9	1	96.97 ± 0.02**	51.51 ± 0.01**	36.37 ± 0.05**	9.09 ± 0.01*	0
	2	100.00 ± 0.00**	5.00 ± 0.02**	90.00 ± 0.07**	5.00 ± 0.03*	0
	4	95.00 ± 0.01**	48.78 ± 0.03**	26.83 ± 0.05**	16.95 ± 0.04**	2.44 ± 0.01
	8	96.67 ± 0.03**	56.67 ± 0.01**	30.00 ± 0.01**	10.00 ± 0.02*	0
	12	100.00 ± 0.00**	52.18 ± 0.04**	38.28 ± 0.01**	4.77 ± 0.03*	4.77 ± 0.02*

[2] S. E., Standard Error * Significant at level P < 0.05 ** Significant at level P < 0.01

12	1	100.00 ± 0.00	52.70 ± 0.03	44.60 ± 0.03	0	2.70 ± 0.01
	2	100.00 ± 0.00	70.00 ± 0.01	30.00 ± 0.01	0	0
	4	**No divided cells (Full inhibition)**				
	8					
	12					

[2] S. E., Standard Error * Significant at level P < 0.05 ** Significant at level P < 0.01

Sticky chromosomes were one of the most often detected abnormalities in root tips of plants treated with ZnO-NPs during metaphase, anaphase, and telophase stages of mitosis (Fig. 9). This finding contradicts the findings of [81, 82], who showed that chromosomal stickiness was the most common CA, and it backs up the significant DNA fragmentation observed in the comet assays conducted by [80, 82] using *A. cepa* specimens. Previously, researchers (83–85], revealed that nanoparticles have the ability to exhibit a wide range of clastogenic effects, including stickiness, aberrant metaphase, and cell wall dissociation, at various exposure dosages. Chromosomal stickiness and other chromosomal anomalies recorded in this study could be due to the ZnO-NPs binding to DNA and proteins and altering their physico-chemical properties, leading to harmful changes in their chromatin structure, nucleus condensation, or the formation of inter- and intra-chromatid crosslinks. This hypothesis is supported by (i) the strong binding affinity of ZnO-NPs for DNA [86], (ii) the formation of ZnO-NPs complexes with the ring N atom or NH site in nucleobases of DNA [87], and (iii) the interaction, as well as the development of a bioconjugate between protein and ZnO-NPs, reported by Bhunia et al. [88], who observed that, the ZnO-NPs induced structural changes/unfolding of protein. Simultaneously, many experts suggested that stickiness indicates a high toxicity of the chemical and leads to abnormal protein-protein interactions [89]. Sticky chromosomes are thought to be a kind of chromatid aberration [90]. Sticky chromosomes are defined by the loss of function of one or two types of particular nonhistone proteins that control chromatid separation and segregation, according to [91]. Stickiness, according to Darlington and McLENH [92], could be caused by chromosomal DNA degradation or depolymerization. Furthermore, the stickiness caused a disruption in the enzyme system, which may have resulted in a reduction in the rate of cell division [93]. The high values of C-metaphases (Fig. 7, 8 and Table 3) show that Zn compounds are aneugenic, which is likely due to disturbance of calmodulin, a tiny Ca^{2+-}binding protein involved in chromosomal mobility via microtubule polymerization/depolymerization regulation [94]. In addition, very high C- mitosis frequencies could imply partial inhibition of the mitotic apparatus due to oxidative stress caused by higher ZnO-NPs concentrations.

There was evidence of structural chromosomal rearrangement and a possible clastogenic character to ZnO-NPs, since chromosomal breakage, ring chromosomes and chromatin bridges were found. During the anaphase stage, chromosomal breakage and disruption were also reported (Fig. 8). The meristematic cells that were exposed to the ZnO-NPs had bridges during anaphase and telophase. The frequency of

micronuclei was seen as a marker for two doses of ZnO-NPs, 4 and 8 PPM, at all times of exposure except at 12 h, when there were no dividing cells, but there were no micronucleated cells in the distilled water as a control.

ZnO-NPs are clearly clastogenic/genotoxic and cytotoxic agents in barley root cells at certain concentrations, as shown by micronucleus. ZnO-NPs exhibited similar genotoxic effects on *A. cepa* and *V. faba*, according to the findings of [80]. In *V. faba* root tip cells, the micronucleus test was utilised by Manzo et al. [95] to investigate the toxicity of ZnO-NPs polluted soil. It has been suggested that micronuclei are formed by chromosomal fragments that do not integrate into either of the daughter nuclei during mitotic telophase, according to [96].

Many different metaphase abnormalities and ana-telophase chromosomal aberrations suggest Zn has genotoxic potential. Chromosome abnormalities indicate that Zn interferes with nucleic acids and has a clastogenic potential.

4 Conclusion

Eco-friendly and low cost effectives for using POP extract as reducing, chelating and capping agents for stabilization and rapid green synthesis ZnO-NPs. Morphological structure, particle size, main groups and crystalline nature were confirmed the nanoscale formation of ZnO-NPs. The biosynthesized ZnO-NPs were assessment for biological activities include antimicrobial, antioxidant, seed germination, root length, shoot height, cytotoxicity and genotoxicity were also the main goals. Data showed that the activities of biosynthesized ZnO-NPs were dose- and time-dependent. The ZnO-NPs exhibit varied activities against the human pathogens used as well as the higher concentrations of ZnO-NPs brought higher shoot length, while root length more significance at 2 PPM of ZnO-NPs. The antioxidant activity of ZnO-NPs observed by IC_{50} = 240 and 250 µg/ml by DPPH and ABTs respectively. From the above findings, it can be confirm the high efficacy of POP extract as a biocatalyst for the green synthesis of ZnO-NPs which used as antimicrobial agent as well as promote the growth of barley in terms of enhanced seeds germination, roots, shoots length and promoting the development of sustainable agriculture and improve the overall yield.

Declarations

Funding sources

This study will be funded through open access by The Science, Technology, and Innovation Funding Authority (STDF) in collaboration with The Egyptian Knowledge Bank (EKB).

Competing Interests

The authors have no relevant financial or non-financial interests to disclose.

Author contributions

Abdelghany S. Shaban was in charge of concept development, methodology, writing- review, and editing. The ZnO-NP was synthesised and characterised by M. E. Owda and Ahmed K. Saleh. The cytogenetics investigation was conducted by Mostafa M. Basyoni and M.A.Mousa. Antimicrobial screening was conducted by Ahmed A. Radwan. Each author contributed to the inquiry and statistics and data analysis in accordance with their role in the methodology. All authors contributed equally to the writing preparation of the initial draught. Supervision was exercised by Abdelghany S. Shaban and Ahmed K. Saleh. The published version of the manuscript has been read and approved by all authors.

Data availability statement

The datasets generated during and/or analysed during the current study are available from the corresponding author on reasonable request.

References

1. R.G. Saratale, G.D. Saratale, H.S. Shin, J.M. Jacob, A. Pugazhendhi, M. Bhaisare, G. Kumar (2018) New insights on the green synthesis of metallic nanoparticles using plant and waste biomaterials: current knowledge, their agricultural and environmental applications, Environ. Sci. Pollut. Res. Int. 25:10164–10183.https://doi.org/10.1007/s11356-017-9912-6
2. R. Sithara, P. Selvakumar, C. Arun, S. Anandan, P. Sivashanmugam (2017) Economical synthesis of silver nanoparticles using leaf extract of Acalypha hispida and its application in the detection of Mn(II) ions, J. Adv. Res. 8:561–568.https://doi.org/10.1016/j.jare.2017.07.001.
3. H. Padalia, S. Chanda (2017) Characterization, antifungal and cytotoxic evaluation of green synthesized zinc oxide nanoparticles using Ziziphus nummularia leaf extract, Artif. Cells Nanomed. Biotechnol. 45 : 1751–1761.https://doi.org/10.1080/21691401.2017.1282868.
4. K. Parveen, V. Banse, L. Ledwani (2016) Green synthesis of nanoparticles: Their advantages and disadvantages, in: American Institute of Physics.
5. R. Yuvakkumar, J. Suresh, A.J. Nathanael, M. Sundrarajan, S.I. Hong (2014) Novel green synthetic strategy to prepare ZnO nanocrystals using rambutan (Nephelium lappaceum L.) peel extract and its antibacterial applications, Mater. Sci. Eng. C Mater. Biol. Appl. 41 :17–27.https://doi.org/10.1016/j.msec.2014.04.025.
6. S. Azizi, M.B. Ahmad, F. Namvar, R. Mohamad (2014) Green biosynthesis and characterization of zinc oxide nanoparticles using brown marine macroalga Sargassum muticum aqueous extract, Mater. Lett. 116:275–277.https://doi.org/10.1016/j.matlet.2013.11.038.
7. H. Abdul Salam, R. Sivaraj, R. Venckatesh (2014) Green synthesis and characterization of zinc oxide nanoparticles from Ocimum basilicum L. var. purpurascens Benth.-Lamiaceae leaf extract, Mater. Lett. 131:16–18.https://doi.org/10.1016/j.matlet.2014.05.033.

8. A. Chaudhary, S. Nandan Rahul (2017) Antibacterial activity of Punica granatum (pomegranate) fruit peel extract against pathogenic and drug resistance bacterial strains, Int. J. Curr. Microbiol. Appl. Sci. 6:3802–3807.https://doi.org/10.20546/ijcmas.2017.612.437.
9. I.A. Adelere, A. Lateef (2016) A novel approach to the green synthesis of metallic nanoparticles: the use of agro-wastes, enzymes, and pigments, Nanotechnol. Rev. 5https://doi.org/10.1515/ntrev-2016-0024.
10. B. Singh, J.P. Singh, A. Kaur, N. Singh (2018) Phenolic compounds as beneficial phytochemicals in pomegranate (Punica granatum L.) peel: A review, Food Chem. 261:75–86.https://doi.org/10.1016/j.foodchem.2018.04.039.
11. X. Fuku, A. Diallo, M. Maaza (2016) Nanoscaled Electrocatalytic Optically Modulated ZnO Nanoparticles through Green Process ofPunica granatumL. and Their Antibacterial Activities, Int. j. Electrochem. 2016:1–10.https://doi.org/10.1155/2016/4682967.
12. M. Nasiriboroumand, M. Montazer, H. Barani (2018) Preparation and characterization of biocompatible silver nanoparticles using pomegranate peel extract, J. Photochem. Photobiol. B. 179 : 98–104.https://doi.org/10.1016/j.jphotobiol.2018.01.006.
13. S. Phongtongpasuk, S. Poadang (2015) Green synthesis of silver nanoparticles using pomegranate peel extract, Adv. Mat. Res. 1131:227–230.https://doi.org/10.4028/www.scientific.net/amr.1131.227.
14. M.E. Vance, T. Kuiken, E.P. Vejerano, S.P. McGinnis, M.F. Hochella Jr, D. Rejeski, M.S. Hull (2015) Nanotechnology in the real world: Redeveloping the nanomaterial consumer products inventory, Beilstein J. Nanotechnol. 6:1769–1780.https://doi.org/10.3762/bjnano.6.181.
15. A. Hussain, S. Ali, M. Rizwan, M. Zia Ur Rehman, M.R. Javed, M. Imran, S.A.S. Chatha, R. Nazir (2018) Zinc oxide nanoparticles alter the wheat physiological response and reduce the cadmium uptake by plants, Environ. Pollut. 242:1518–1526.https://doi.org/10.1016/j.envpol.2018.08.036.
16. G. de la Rosa, M.L. López-Moreno, D. de Haro, C.E. Botez, J.R. Peralta-Videa, J.L. Gardea-Torresdey (2013) Effects of ZnO nanoparticles in alfalfa, tomato, and cucumber at the germination stage: Root development and X-ray absorption spectroscopy studies, Pure Appl. Chem. 85:2161–2174.https://doi.org/10.1351/pac-con-12-09-05.
17. B. Kumari, K.V. Rao (2014) Germination and Growth Characteristics of Mungbean Seeds (Vigna radiata L.) affected by Synthesized Zinc Oxide Nanoparticles, Int. J. Curr. Eng. Technol.4:2347-5161.
18. M. Rizwan, S. Ali, M.F. Qayyum, Y.S. Ok, M. Adrees, M. Ibrahim, M. Zia-ur-Rehman, M. Farid, F. Abbas (2017) Effect of metal and metal oxide nanoparticles on growth and physiology of globally important food crops: A critical review, J. Hazard. Mater. 322:2–16.https://doi.org/10.1016/j.jhazmat.2016.05.061.
19. A. Misra, A.K. Srivastava, N.K. Srivastava, A. Khan (2005) Zn-acquisition and its role in growth, photosynthesis, photosynthetic pigments, and biochemical changes in essential monoterpene oil(s) of Pelargonium graveolens, Photosynthetica. 43:153–155.https://doi.org/10.1007/s11099-005-3155-3.

20. H.R. Eisvand, H. Kamaei, F. Nazarian (2018) Chlorophyll fluorescence, yield and yield components of bread wheat affected by phosphate bio-fertilizer, zinc and boron under late-season heat stress, Photosynthetica. 56:1287–1296.https://doi.org/10.1007/s11099-018-0829-1.
21. T. Tsonev, F. Lidon (2012) Zinc in plants - an overview, Emirates Journal of Food and Agriculture; Al-Ain. 24: 322–333. https://www.semanticscholar.org/paper/ffe51c83531acbf1a2d985fa061f10d069105176 (accessed January 29, 2022).
22. M. Sedghi, M. Hadi, S.G. Toluie (2013) Effect of nano zinc oxide on the germination parameters of soybean seeds under drought stress, Ann. West Univ. Timiş. 16:73–78.https://www.ingentaconnect.com/content/doaj/15823830/2013/00000016/00000002/art00002.
23. R. Szőllősi, Á. Molnár, S. Kondak, Z. Kolbert (2020) Dual effect of nanomaterials on germination and seedling growth: Stimulation vs. Phytotoxicity, Plants. 9:1745.https://doi.org/10.3390/plants9121745.
24. R. Kaveh, Y.-S. Li, S. Ranjbar, R. Tehrani, C.L. Brueck, B. Van Aken (2013) Changes in Arabidopsis thaliana gene expression in response to silver nanoparticles and silver ions, Environ. Sci. Technol. 47:10637–10644.https://doi.org/10.1021/es402209w.
25. M. Ghosh, I. Ghosh, L. Godderis, P. Hoet, A. Mukherjee (2019) Genotoxicity of engineered nanoparticles in higher plants, Mutat. Res. Genet. Toxicol. Environ. Mutagen. 842:132–145.https://doi.org/10.1016/j.mrgentox.2019.01.002.
26. N.V. Long, O. Dolstra, M. Malosetti, B. Kilian, A. Graner, R.G.F. Visser, C.G. van der Linden (2013) Association mapping of salt tolerance in barley (*Hordeum vulgare*L.), Züchter Genet. Breed. Res. 126:2335–2351.https://doi.org/10.1007/s00122-013-2139-0.
27. A. Mattiello, A. Filippi, F. Pošćić, R. Musetti, M.C. Salvatici, C. Giordano, M. Vischi, A. Bertolini, L. Marchiol (2015) Evidence of phytotoxicity and genotoxicity in *Hordeum vulgare*L. exposed to CeO2 and TiO2 nanoparticles, Front. Plant Sci. 6:1043.https://doi.org/10.3389/fpls.2015.01043.
28. J. Ferdous, Y. Li, N. Reid, P. Langridge, B.-J. Shi, P.J. Tricker (2015) Identification of reference genes for quantitative expression analysis of microRNAs and mRNAs in barley under various stress conditions, PLoS One. 10:e0118503.https://doi.org/10.1371/journal.pone.0118503.
29. J. Bian, P. Deng, H. Zhan, X. Wu, M.D.L.C. Nishantha, Z. Yan, X. Du, X. Nie, W. Song (2019) Transcriptional dynamics of grain development in barley (*Hordeum vulgare*L.), Int. J. Mol. Sci. 20:962.https://doi.org/10.3390/ijms20040962.
30. S. Dwivedi, R. Wahab, F. Khan, Y.K. Mishra, J. Musarrat, A.A. Al-Khedhairy (2014) Reactive oxygen species mediated bacterial biofilm inhibition via zinc oxide nanoparticles and their statistical determination, PLoS One. 9:e111289.https://doi.org/10.1371/journal.pone.0111289.
31. F. Ghasemi, R. Jalal (2016) Antimicrobial action of zinc oxide nanoparticles in combination with ciprofloxacin and ceftazidime against multidrug-resistant Acinetobacter baumannii, J. Glob. Antimicrob. Resist. 6:118–122.https://doi.org/10.1016/j.jgar.2016.04.007.

32. M. Patel, N.J. Siddiqi, P. Sharma, A.S. Alhomida, H.A. Khan (2019) Reproductive toxicity of pomegranate peel extract synthesized gold nanoparticles: A multigeneration study in C. elegans, J. Nanomater. 2019: 1–7.https://doi.org/10.1155/2019/8767943.
33. P.A. Wayne (2011) Clinical And Laboratory Standards Institute. Performance standards for antimicrobial susceptibility testing, 31:100–121. https://www.sid.ir/en/Journal/ViewPaper.aspx?ID=450165 (accessed January 29, 2022).
34. S. Magaldi, S. Mata-Essayag, C. Hartung de Capriles, C. Perez, M.T. Colella, C. Olaizola, Y. Ontiveros (2004) Well diffusion for antifungal susceptibility testing, Int. J. Infect. Dis. 8:39–45.https://doi.org/10.1016/j.ijid.2003.03.002.
35. M.H. Sharaf, A.M. Abdelaziz, M.H. Kalaba, A.A. Radwan, A.H. Hashem (2021) Antimicrobial, antioxidant, cytotoxic activities and phytochemical analysis of fungal endophytes isolated from Ocimum Basilicum, Appl. Biochem. Biotechnol. 1-19.https://doi.org/10.1007/s12010-021-03702-w.
36. K.J. Lee, Y.C. Oh, W.K. Cho, J.Y. Ma (2015) Antioxidant and anti-inflammatory activity determination of one hundred kinds of pure chemical compounds using offline and online screening HPLC assay, Evid. Based. Complement. Alternat. Med. 2015, 165457.https://doi.org/10.1155/2015/165457.
37. A. Özkara, D. Akyıl, S.F. Erdoğmuş, M. Konuk(2011) Evaluation of germination, root growth and cytological effects of wastewater of sugar factory (Afyonkarahisar) using *Hordeum vulgare*bioassays, Environ. Monit. Assess. 183:517–524.https://doi.org/10.1007/s10661-011-1936-7.
38. Y. Hu, L. Tan, S.-H. Zhang, Y.-T. Zuo, X. Han, N. Liu, W.-Q. Lu, A.-L. Liu (2017) Detection of genotoxic effects of drinking water disinfection by-products using Vicia faba bioassay, Environ. Sci. Pollut. Res. Int. 24:1509–1517.https://doi.org/10.1007/s11356-016-7873-9.
39. A. Kołodziejczak-Radzimska, E. Markiewicz, T. Jesionowski (2012) Structural characterisation of ZnO particles obtained by the emulsion precipitation method, J. Nanomater. 2012:1–9.https://doi.org/10.1155/2012/656353.
40. M. Shabaani, S. Rahaiee, M. Zare, S.M. Jafari (2020) Green synthesis of ZnO nanoparticles using loquat seed extract; Biological functions and photocatalytic degradation properties, Lebenson. Wiss. Technol. 134:110133.https://doi.org/10.1016/j.lwt.2020.110133.
41. A.M. Awwad, N.M. Salem, A.O. Abdeen (2012) Biosynthesis of Silver Nanoparticles using *Olea europaea* Leaves Extract and its Antibacterial Activity, Nanosci. Nanotechnol. 2:164–170. http://article.sapub.org/10.5923.j.nn.20120206.03.html (accessed January 29, 2022).
42. S. Mukherjee, V. Sushma, S. Patra, A.K. Barui, M.P. Bhadra, B. Sreedhar, C.R. Patra (2012) Green chemistry approach for the synthesis and stabilization of biocompatible gold nanoparticles and their potential applications in cancer therapy, Nanotechnology. 23:455103.https://doi.org/10.1088/0957-4484/23/45/455103.
43. G. Sharmila, M. Thirumarimurugan, C. Muthukumaran (2019) Green synthesis of ZnO nanoparticles using Tecoma castanifolia leaf extract: Characterization and evaluation of its antioxidant,

bactericidal and anticancer activities, Microchem. J. 145 578–587.https://doi.org/10.1016/j.microc.2018.11.022.

44. V. Tiwari, N. Mishra, K. Gadani, P.S. Solanki, N.A. Shah, M. Tiwari (2018) Mechanism of anti-bacterial activity of zinc oxide nanoparticle against carbapenem-resistant Acinetobacter baumannii, Front. Microbiol. 9:1218.https://doi.org/10.3389/fmicb.2018.01218.
45. M. Saliani, R. Jalal, E. Kafshdare Goharshadi (2015) Effects of pH and temperature on antibacterial activity of zinc oxide nanofluid against Escherichia coli O157: H7 and Staphylococcus aureus, Jundishapur J. Microbiol. 8: e17115.https://doi.org/10.5812/jjm.17115.
46. J. Ali, R. Irshad, B. Li, K. Tahir, A. Ahmad, M. Shakeel, N.U. Khan, Z.U.H. Khan (2018) Synthesis and characterization of phytochemical fabricated zinc oxide nanoparticles with enhanced antibacterial and catalytic applications, J. Photochem. Photobiol. B. 183:349–356.https://doi.org/10.1016/j.jphotobiol.2018.05.006.
47. L. Wang, C. Hu, L. Shao (2017) The antimicrobial activity of nanoparticles: present situation and prospects for the future, Int. J. Nanomedicine. 12:1227–1249.https://doi.org/10.2147/IJN.S121956.
48. M.H. Kalaba, S.A. Moghannem, A.S. El-Hawary, A.A. Radwan, M.H. Sharaf, A.S. Shaban (2021) Green synthesized ZnO nanoparticles mediated by Streptomyces plicatus: Characterizations, antimicrobial and nematicidal activities and cytogenetic effects, Plants. 10 :1760.https://doi.org/10.3390/plants10091760.
49. S. Shaikh, N. Nazam, S.M.D. Rizvi, K. Ahmad, M.H. Baig, E.J. Lee, I. Choi (2019) Mechanistic insights into the antimicrobial actions of metallic nanoparticles and their implications for multidrug resistance, Int. J. Mol. Sci. 20:2468.https://doi.org/10.3390/ijms20102468.
50. L. He, Y. Liu, A. Mustapha, M. Lin (2011) Antifungal activity of zinc oxide nanoparticles against Botrytis cinerea and Penicillium expansum, Microbiol. Res. 166:207–215.https://doi.org/10.1016/j.micres.2010.03.003.
51. J.H. Lee, B.W. Lee, B. Kim, H.T. Kim, J.M. Ko, I.-Y. Baek, W.T. Seo, Y.M. Kang, K.M. Cho (2013) Changes in phenolic compounds (Isoflavones and Phenolic acids) and antioxidant properties in high-protein soybean (Glycine max L., cv. Saedanbaek) for different roasting conditions, J Korean Soc Appl Biol Chem. 56:605–612.https://doi.org/10.1007/s13765-013-3048-2.
52. E.B. Kurutas (2015) The importance of antioxidants which play the role in cellular response against oxidative/nitrosative stress: current state, Nutr. J. 15: 1-22.https://doi.org/10.1186/s12937-016-0186-5.
53. L. Xiang, H.-M. Zhao, Y.-W. Li, X.-P. Huang, X.-L. Wu, T. Zhai, Y. Yuan, Q.-Y. Cai, C.-H. Mo (2015) Effects of the size and morphology of zinc oxide nanoparticles on the germination of Chinese cabbage seeds, Environ. Sci. Pollut. Res. Int. 22:10452–10462.https://doi.org/10.1007/s11356-015-4172-9.
54. I. Plaksenkova, I. Kokina, A. Petrova, M. Jermaļonoka, V. Gerbreders, M. Krasovska (2020) The impact of zinc oxide nanoparticles on cytotoxicity, genotoxicity, and miRNA expression in barley (*Hordeum vulgare*L.) seedlings, ScientificWorldJournal. 2020:6649746.https://doi.org/10.1155/2020/6649746.

55. Upadhyaya (2017) Physiological impact of Zinc nanoparticle on germination of rice (Oryza sativa L) seed, J. Plant Sci. Phytopathol. 1: 062–070.https://doi.org/10.29328/journal.jpsp.1001008.
56. R. Raliya, R. Nair, S. Chavalmane, W.-N. Wang, P. Biswas (2015) Mechanistic evaluation of translocation and physiological impact of titanium dioxide and zinc oxide nanoparticles on the tomato (Solanum lycopersicum L.) plant, Metallomics. 7: 1584–1594.https://doi.org/10.1039/c5mt00168d.
57. R. Zhang, H. Zhang, C. Tu, X. Hu, L. Li, Y. Luo, P. Christie (2015) Phytotoxicity of ZnO nanoparticles and the released Zn(II) ion to corn (Zea mays L.) and cucumber (Cucumis sativus L.) during germination, Environ. Sci. Pollut. Res. Int. 22: 11109–11117.https://doi.org/10.1007/s11356-015-4325-x.
58. S. Adhikari, A. Adhikari, S. Ghosh, D. Roy, I. Azahar, D. Basuli, Z. Hossain, (2020) Assessment of ZnO-NPs toxicity in maize: An integrative microRNAomic approach, Chemosphere. 249:126197.https://doi.org/10.1016/j.chemosphere.2020.126197.
59. R. Raliya, J.C. Tarafdar (2013) ZnO nanoparticle biosynthesis and its effect on phosphorous-mobilizing enzyme secretion and gum contents in clusterbean (Cyamopsis tetragonoloba L.), Agric. Res. 2:48–57.https://doi.org/10.1007/s40003-012-0049-z.
60. R. Raliya, R. Nair, S. Chavalmane, W.-N. Wang, P. Biswas (2015) Mechanistic evaluation of translocation and physiological impact of titanium dioxide and zinc oxide nanoparticles on the tomato (Solanum lycopersicum L.) plant, Metallomics. 7:1584–1594.https://doi.org/10.1039/c5mt00168d.
61. L. Yang, D.J. Watts (2005) Particle surface characteristics may play an important role in phytotoxicity of alumina nanoparticles, Toxicol. Lett. 158:122–132.https://doi.org/10.1016/j.toxlet.2005.03.003.
62. D. Lin, B. Xing (2007) Phytotoxicity of nanoparticles: inhibition of seed germination and root growth, Environ. Pollut. 150:243–250.https://doi.org/10.1016/j.envpol.2007.01.016.
63. O. Munzuroglu, H. Geckil (2002) Effects of metals on seed germination, root elongation, and coleoptile and hypocotyl growth in Triticum aestivum and Cucumis sativus, Arch. Environ. Contam. Toxicol. 43: 203–213.https://doi.org/10.1007/s00244-002-1116-4.
64. X. Wang, C. Sun, S. Gao, L. Wang, H. Shuokui (2001) Validation of germination rate and root elongation as indicator to assess phytotoxicity with Cucumis sativus, Chemosphere. 441:711–1721.https://doi.org/10.1016/s0045-6535(00)00520-8.
65. M. Faizan, A. Faraz, M. Yusuf, S.T. Khan, S. Hayat (2018) Zinc oxide nanoparticle-mediated changes in photosynthetic efficiency and antioxidant system of tomato plants, Photosynthetica. 56:678–686.https://doi.org/10.1007/s11099-017-0717-0.
66. K. Linnainmaa, T. Meretoja, M. Sorsa, H. Vainio (1978) Cytogenetic effects of styrene and styrene oxide, Mutat. Res.-Rev. Genet. Toxicol. 58:277–286.https://doi.org/10.1016/0165-1218(78)90020-4.
67. A. Tymoszuk, J. Wojnarowicz (2020) Zinc oxide and zinc oxide nanoparticles impact on in vitro germination and seedling growth in Allium cepa L, Materials (Basel). 13 :2784.https://doi.org/10.3390/ma13122784.

68. T. Shaymurat, J. Gu, C. Xu, Z. Yang, Q. Zhao, Y. Liu, Y. Liu (2012) Phytotoxic and genotoxic effects of ZnO nanoparticles on garlic (*Allium sativum* L.): a morphological study, Nanotoxicology. 6:241–248.https://doi.org/10.3109/17435390.2011.570462.

69. T.N.V.K.V. Prasad, P. Sudhakar, Y. Sreenivasulu, P. Latha, V. Munaswamy, K.R. Reddy, T.S. Sreeprasad, P.R. Sajanlal, T. Pradeep (2012) Effect of nanoscale zinc oxide particles on the germination, growth and yield of peanut, J. Plant Nutr. 35:905–927.https://doi.org/10.1080/01904167.2012.663443.

70. Y.-F. Lin, M.G.M. Aarts (2012) The molecular mechanism of zinc and cadmium stress response in plants, Cell. Mol. Life Sci. 69:3187–3206.https://doi.org/10.1007/s00018-012-1089-z.

71. O.B. Nalci, H. Nadaroglu, A.H. Pour, A.A. Gungor, K. Haliloglu (2019) Effects of ZnO, CuO and γ-Fe3O4 nanoparticles on mature embryo culture of wheat (Triticum aestivum L.), Plant Cell Tissue Organ Cult. 136:269–277.https://doi.org/10.1007/s11240-018-1512-8.

72. L. Giorgetti, H. Talouizte, M. Merzouki, L. Caltavuturo, C. Geri, S. Frassinetti (2011) Genotoxicity evaluation of effluents from textile industries of the region Fez-Boulmane, Morocco: a case study, Ecotoxicol. Environ. Saf. 74:2275–2283.https://doi.org/10.1016/j.ecoenv.2011.08.002.

73. M. Barbafieri, L. Giorgetti (2016) Contaminant bioavailability in soil and phytotoxicity/genotoxicity tests in Vicia faba L.: a case study of boron contamination, Environ. Sci. Pollut. Res. Int. 23:24327–24336.https://doi.org/10.1007/s11356-016-7653-6.

74. M. Ruffini Castiglione, L. Giorgetti, R. Cremonini, S. Bottega, C. Spanò (2014) Impact of TiO nanoparticles on Vicia narbonensis L.: potential toxicity effects, Protoplasma. 251:1471–1479.https://doi.org/10.1007/s00709-014-0649-5.

75. M. Ruffini Castiglione, L. Giorgetti, S. Becarelli, G. Siracusa, R. Lorenzi, S. Di Gregorio (2016) Polycyclic aromatic hydrocarbon-contaminated soils: bioaugmentation of autochthonous bacteria and toxicological assessment of the bioremediation process by means of Vicia faba L, Environ. Sci. Pollut. Res. Int. 23:7930–7941.https://doi.org/10.1007/s11356-016-6049-y.

76. M. Kumari, S.S. Khan, S. Pakrashi, A. Mukherjee, N. Chandrasekaran (2011) Cytogenetic and genotoxic effects of zinc oxide nanoparticles on root cells of Allium cepa, J. Hazard. Mater. 190:613–621.https://doi.org/10.1016/j.jhazmat.2011.03.095.M.S.

77. Youssef, R.M. Elamawi (2020) Evaluation of phytotoxicity, cytotoxicity, and genotoxicity of ZnO nanoparticles in Vicia faba, Environ. Sci. Pollut. Res. Int. 27:18972–18984.https://doi.org/10.1007/s11356-018-3250-1.

78. T.C. Taranath, B.N. Patil, T.U. Santosh, B.S. Sharath (2015) Cytotoxicity of zinc nanoparticles fabricated by Justicia adhatoda L. on root tips of Allium cepa L.–a model approach, Environ. Sci. Pollut. Res. Int. 22:8611–8617.https://doi.org/10.1007/s11356-014-4043-9.

79. A.A. El-Ghamery, A.I. El-Nahas, M.M. Mansour (2000) The action of atrazine herbicide as an inhibitor of cell division on chromosomes and nucleic acids content in root meristems of Allium cepa and Vicia faba, Cytologia (Tokyo). 65:277–287.https://doi.org/10.1508/cytologia.65.277.

80. M. Ghosh, A. Jana, S. Sinha, M. Jothiramajayam, A. Nag, A. Chakraborty, A. Mukherjee, A. Mukherjee (2016) Effects of ZnO nanoparticles in plants: Cytotoxicity, genotoxicity, deregulation of antioxidant

defenses, and cell-cycle arrest, Mutat. Res. Genet. Toxicol. Environ. Mutagen. 807:25–32.https://doi.org/10.1016/j.mrgentox.2016.07.006.

81. M. Kumari, A. Mukherjee, N. Chandrasekaran (2009) Genotoxicity of silver nanoparticles in Allium cepa, Sci. Total Environ. 407:5243–5246.https://doi.org/10.1016/j.scitotenv.2009.06.024.
82. Z. Sun, T. Xiong, T. Zhang, N. Wang, D. Chen, S. Li (2019) Influences of zinc oxide nanoparticles on Allium cepa root cells and the primary cause of phytotoxicity, Ecotoxicology. 28:175–188.https://doi.org/10.1007/s10646-018-2010-9.
83. K. Krishnamoorthy, J.Y. Moon, H.B. Hyun, S.K. Cho, S.-J. Kim (2012) Mechanistic investigation on the toxicity of MgO nanoparticles toward cancer cells, J. Mater. Chem. 22:24610–24617.https://doi.org/10.1039/C2JM35087D.
84. S. Bakand, A. Hayes (2016) Toxicological considerations, toxicity assessment, and risk management of inhaled nanoparticles, Int. J. Mol. Sci. 17: 929.https://doi.org/10.3390/ijms17060929.
85. B. Ahmed, M. Shahid, M.S. Khan, J. Musarrat (2018) Chromosomal aberrations, cell suppression and oxidative stress generation induced by metal oxide nanoparticles in onion (Allium cepa) bulb, Metallomics. 10:1315–1327.https://doi.org/10.1039/c8mt00093j.
86. S. Das, S. Chatterjee, S. Pramanik, P.S. Devi, G.S. Kumar (2018) A new insight into the interaction of ZnO with calf thymus DNA through surface defects, J. Photochem. Photobiol. B. 178:339–347.https://doi.org/10.1016/j.jphotobiol.2017.10.039.
87. S. Saha, P. Sarkar (2014) Understanding the interaction of DNA-RNA nucleobases with different ZnO nanomaterials, Phys. Chem. Chem. Phys. 16:15355–15366.https://doi.org/10.1039/c4cp01041h.
88. A.K. Bhunia, P.K. Samanta, S. Saha, T. Kamilya (2013) ZnO nanoparticle-protein interaction: Corona formation with associated unfolding, Appl. Phys. Lett. 103:143701.https://doi.org/10.1063/1.4824021.
89. N.M.C. Nwakanma, B.E. Okoli (2010) Cytological effects of the root extracts of Boerhaavia diffusa on root tips of Crinum jagus, Eurasian J. Biosci. 105–111.https://doi.org/10.5053/ejobios.2010.4.0.13.
90. A. Badr (1986) Effects of the s-triazine herbicide turbutryn on mitosis, chromosomes and nucleic acids in root tips of Vicia faba, Cytologia (Tokyo). 51:571–577.https://doi.org/10.1508/cytologia.51.571.
91. M.E. Gaulden (1987) Hypothesis: some mutagens directly alter specific chromosomal proteins (DNA topoisomerase II and peripheral proteins) to produce chromosome stickiness, which causes chromosome aberrations, Mutagenesis. 2:357–365.https://doi.org/10.1093/mutage/2.5.357.
92. C.D. Darlington, J. McLENH (1951) Action of maleic hydrazide on the cell, Nature. 167:407–408.https://doi.org/10.1038/167407a0.
93. L., Mahakhode (2013) Mitotic abnormalities induced by glyphosate in Psoralea corylifolia l, International Journal of Current Pharmaceutical Research. 5:46-48. https://www.semanticscholar.org/paper/e67d54fe81f99df5d5104091324a88eaf1d6e45c (accessed January 31, 2022).

94. J. Zou, M. Wang, W. Jiang, D. Liu (2006) Effects of hexavalent chromium (VI) on root growth and cell division in root tip cells of Amaranthus viridis L, Pakistan Journal of Botany. 38:673. https://www.semanticscholar.org/paper/d8212676314bfc80c442cb74361023f2ba51c825 (accessed January 31, 2022).
95. S. Manzo, A. Rocco, R. Carotenuto, F.D.L. Picione, M.L. Miglietta, G. Rametta, G. Di Francia (2011) Investigation of ZnO nanoparticles' ecotoxicological effects towards different soil organisms, Environ. Sci. Pollut. Res. Int. 18:756–763.https://doi.org/10.1007/s11356-010-0421-0.
96. G. Krishna, M. Hayashi (2000) In vivo rodent micronucleus assay: protocol, conduct and data interpretation, Mutat. Res. 455:155–166.https://doi.org/10.1016/s0027-5107(00)00117-2.

Figures

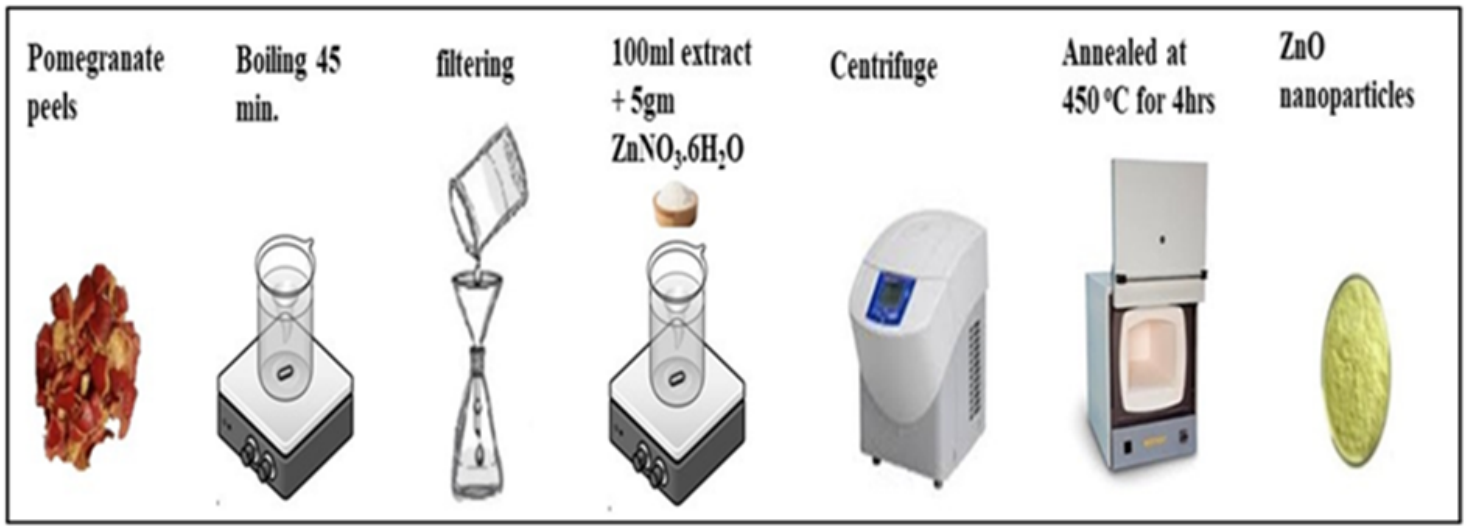

Figure 1

Green synthesis of ZnO-NPs using POP extract

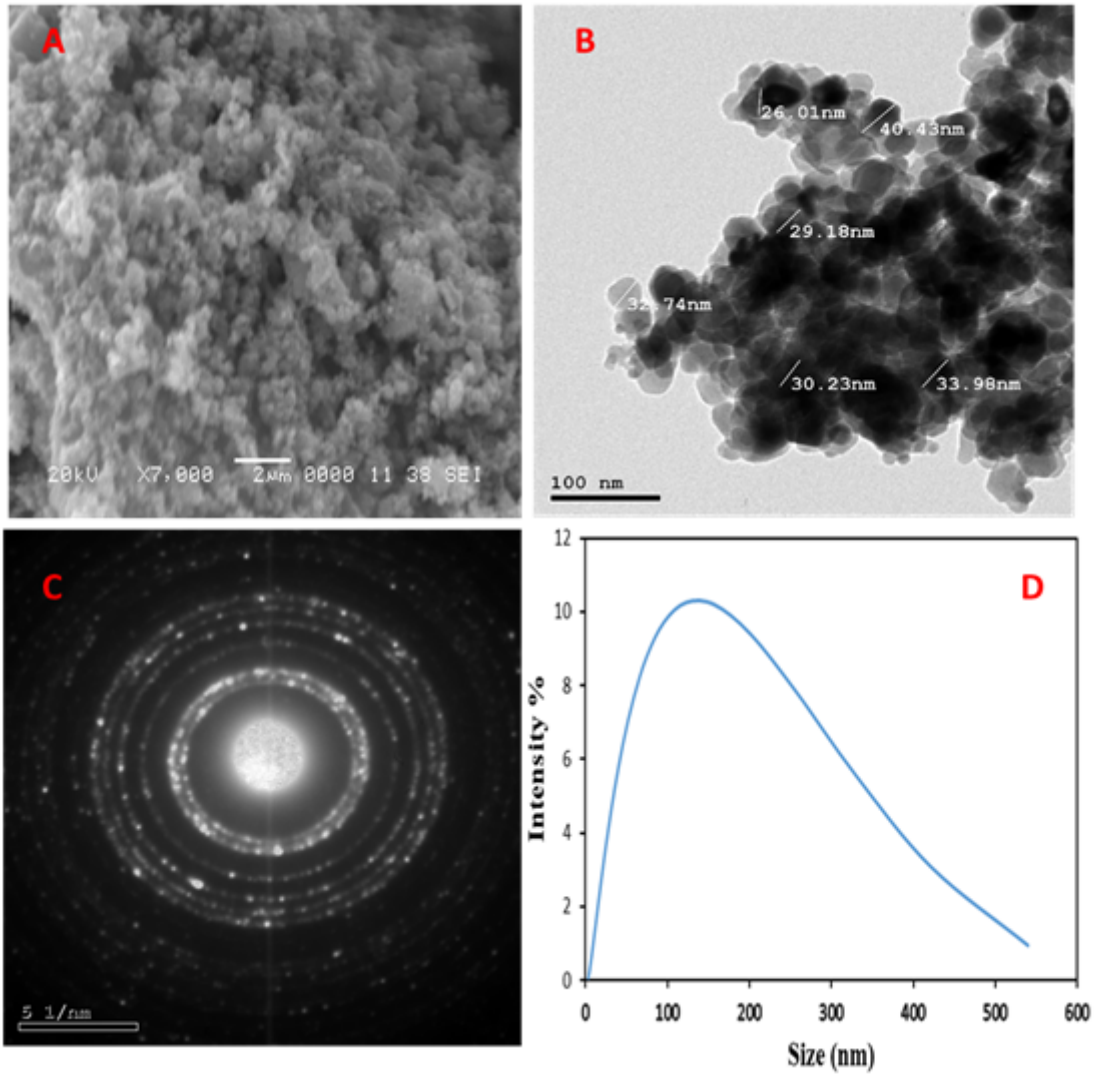

Figure 2

characterization of the biosynthesized ZnO-NPs A) denotes SEM image, B) denotes TEM image, C) SAED pattern of ZnO-NPs (C), and D) particle size distribution.

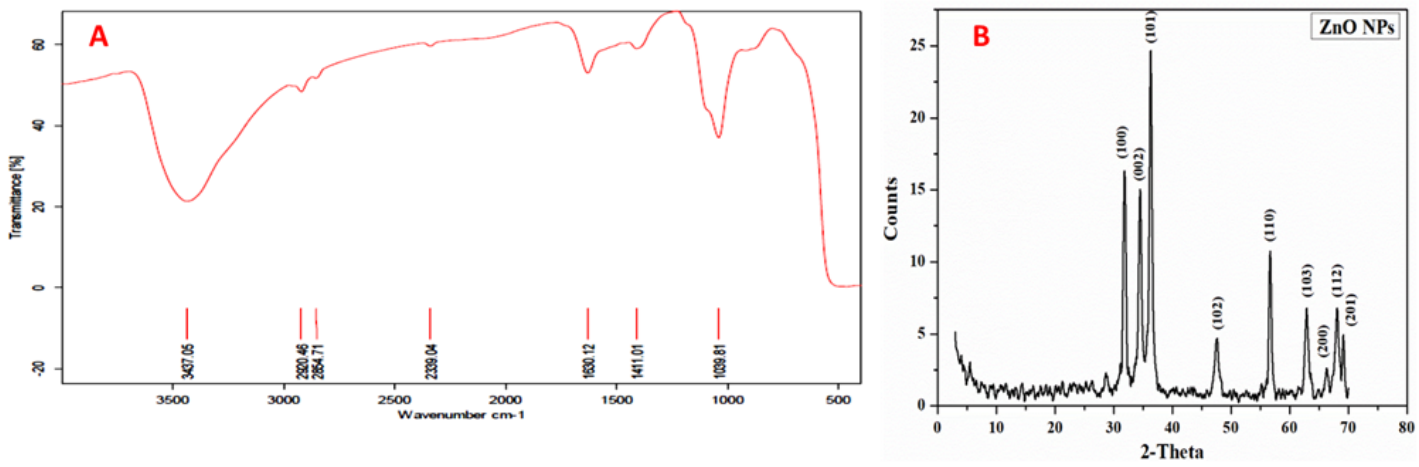

Figure 3

A) FT-IR spectra, and B) XRD of the synthesized ZnO-NPs.

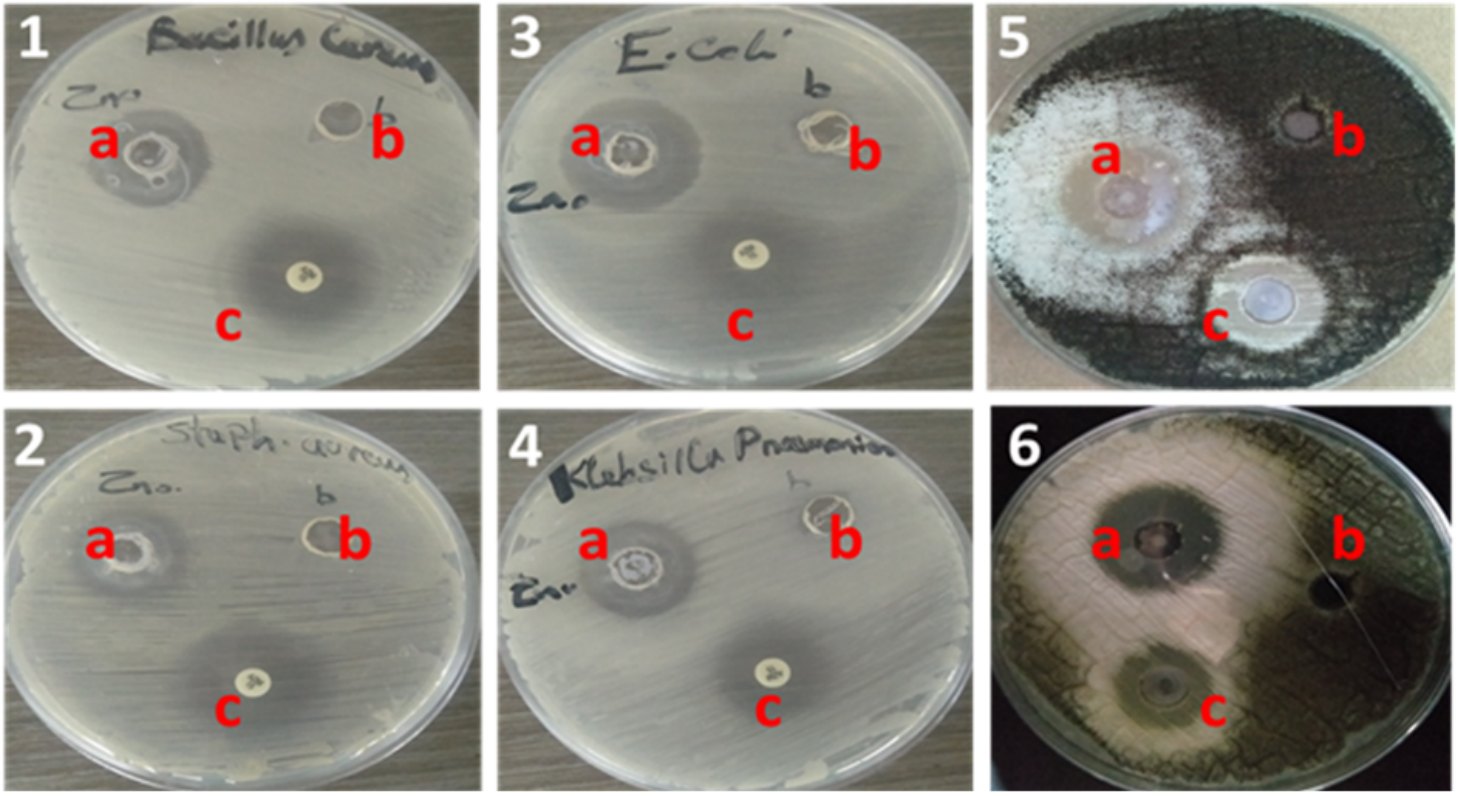

Figure 4

The antimicrobial activity of biosynthesized ZnO-NPs against (1: B. cereus, 2: S. aureus, 3: E. coli, 4: K. pneumonia, 5: A. niger and 6: A. flavus), different letters (a, b, and c) match ZnO-NPs nanofluid.

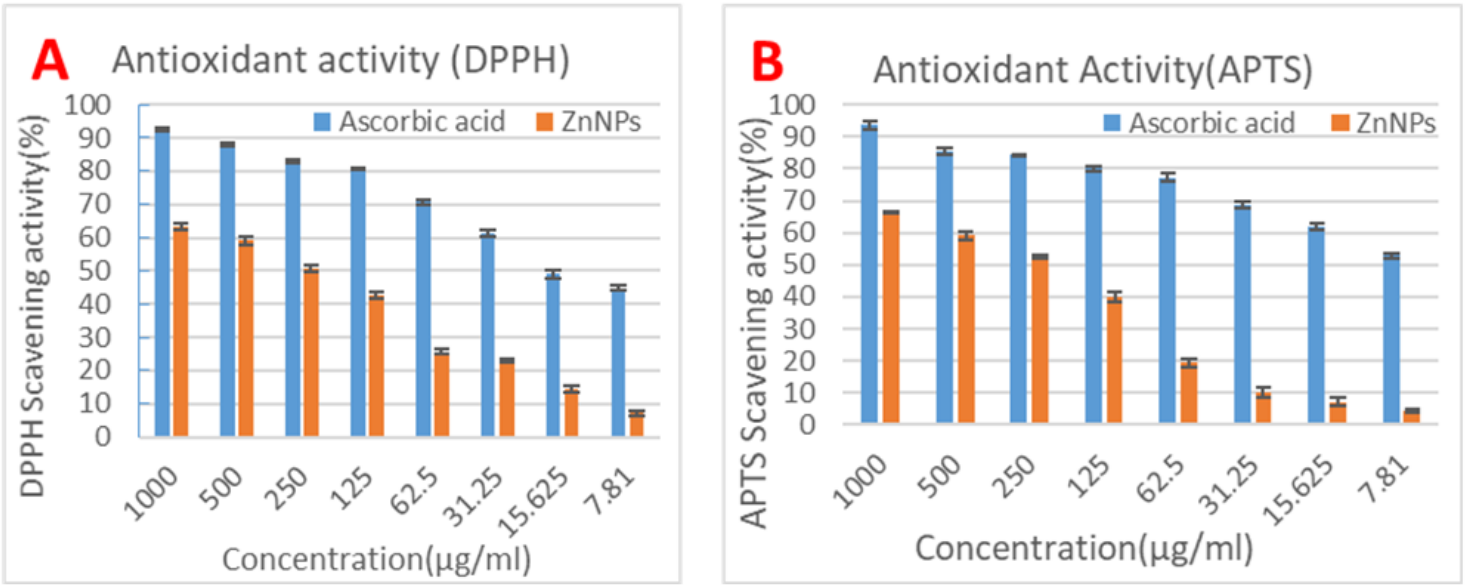

Figure 5

Antioxidant activity of ZnO-NPs at different concentrations by DPPH and APTS.

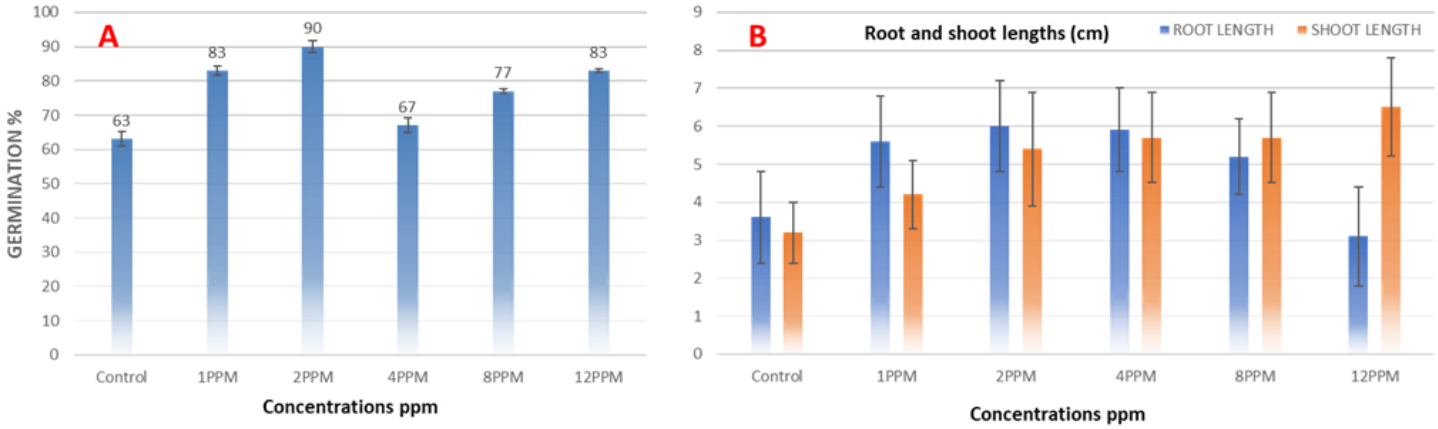

Figure 6

The effects of varying ZnO-NP concentrations on the growth of Hordeum vulgare, (a) the percentage of seeds that germinate; (b) the lengths of shoots and roots (cm).

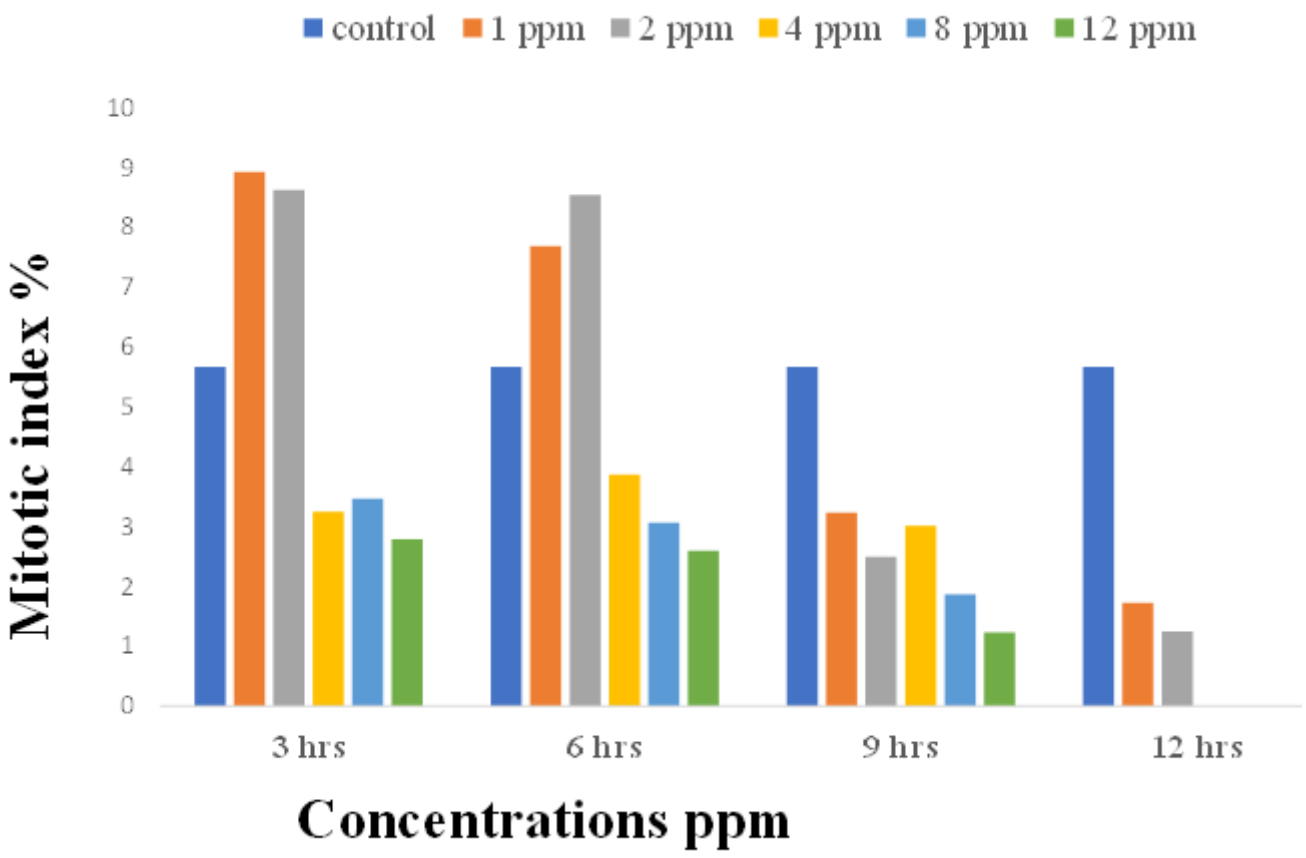

Figure 7

Mitotic index as a result of the cytotoxic action of ZnO-NPs on barley root meristems

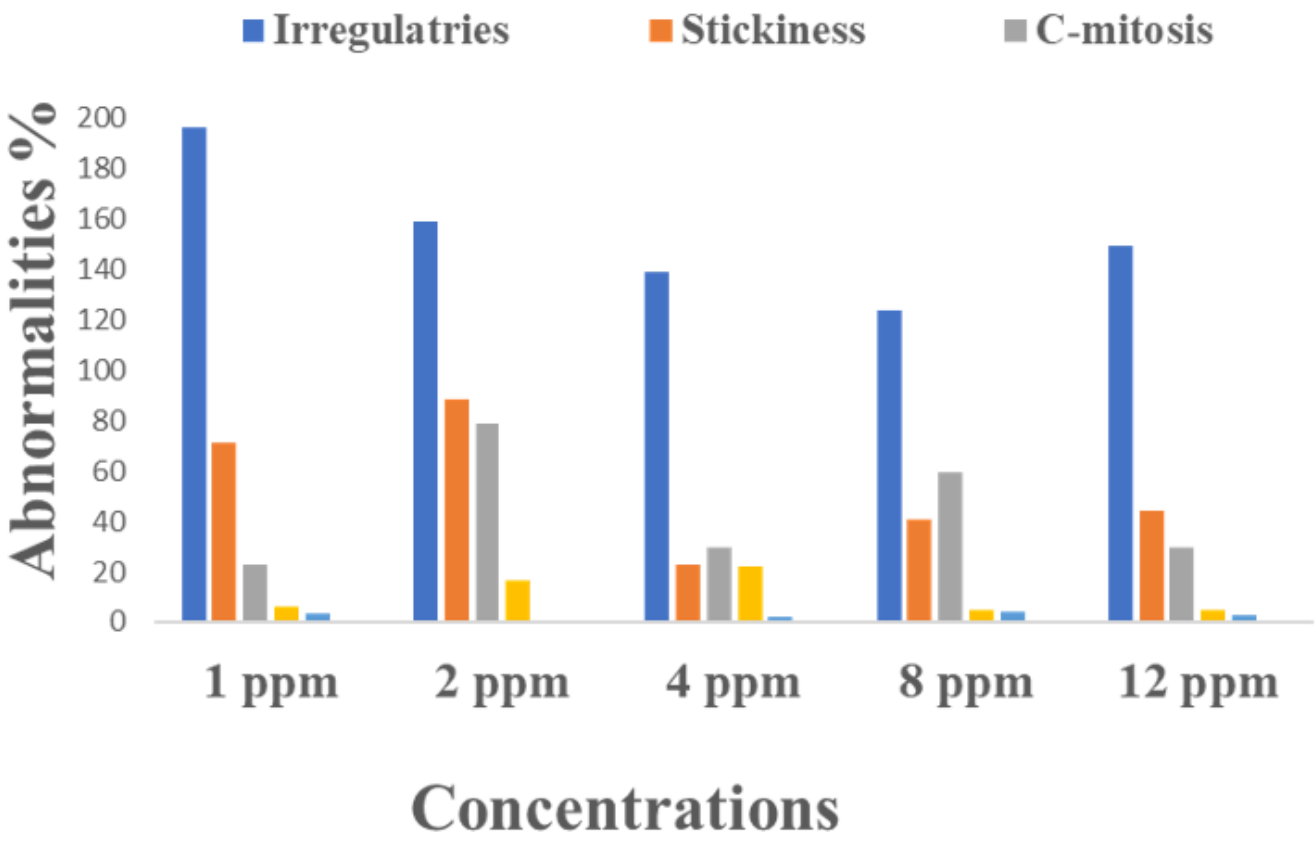

Figure 8

Cytotoxic effect of ZnO-NPs on root meristems of barley; % of most chromosomal abnormalities.

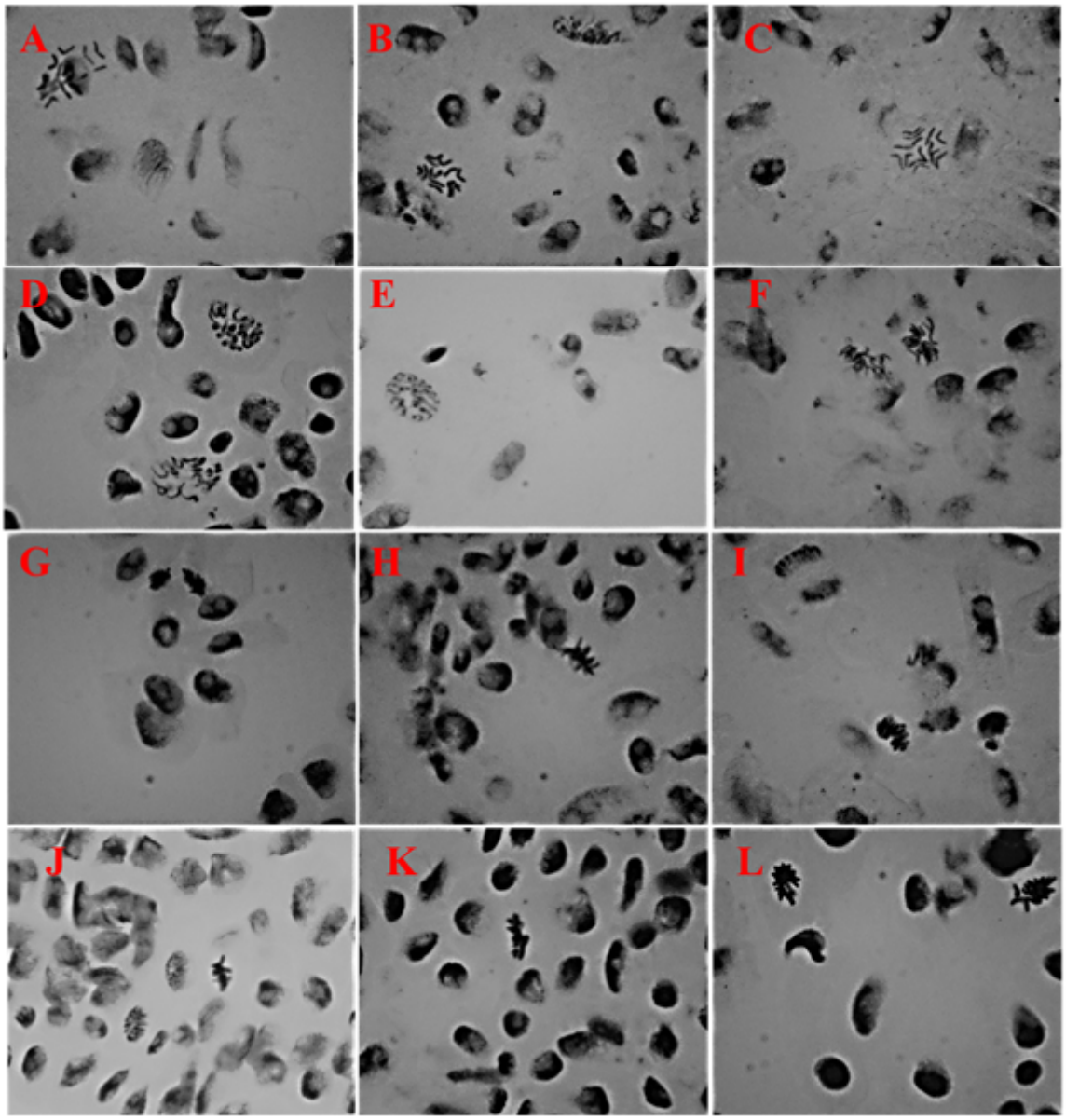

Figure 9

Different treatments of ZnO-NPs caused abnormalities in barley root meristems: (A-C) C- metaphase; (D,E) irregular, granulated, and vacuolated prophase; (F) laggard at metaphase; (G- k) sticky metaphase; (L) Metaphase with 2 lagging chromosomes;(M,O)st